UCRL-JC-134883
PREPRINT

Thomson Scattering from Inertial Confinement Fusion Targets

Siefried H. Glenzer

This paper was prepared for submittal to the
9th International Symposium on Laser-Aided Plasma Diagnostics
Lake Tahoe, California
September 26 - October 1, 1999

July 22, 1999

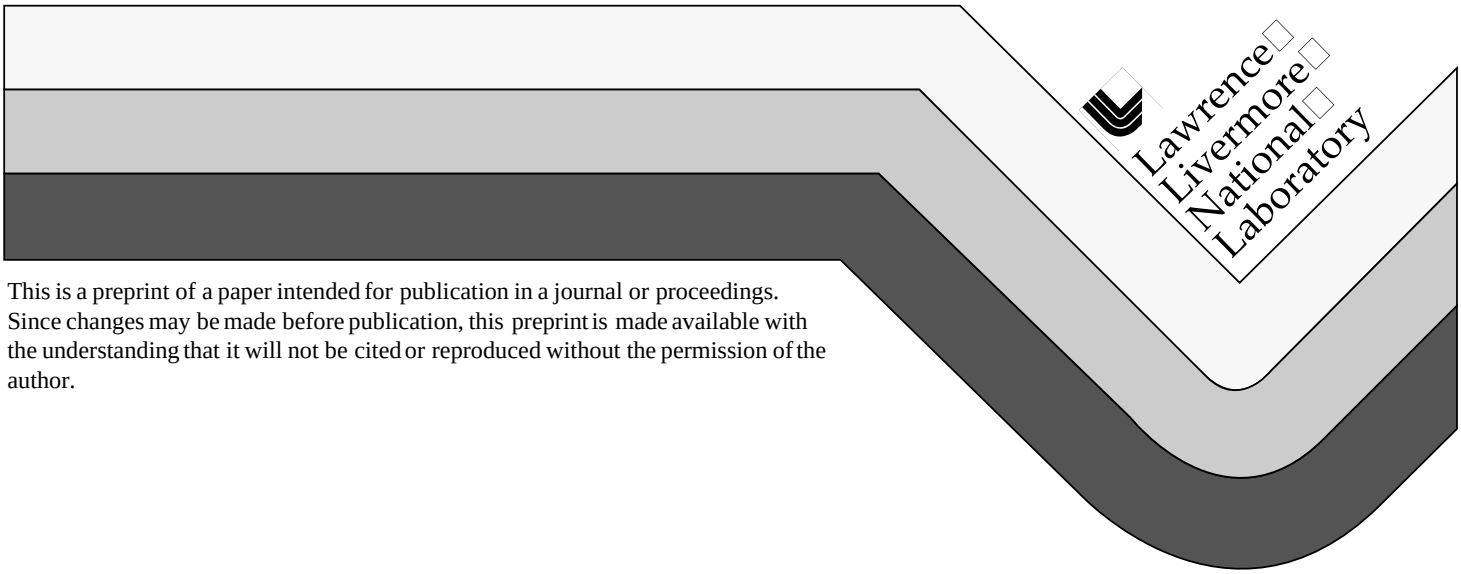

THOMSON SCATTERING FROM INERTIAL CONFINEMENT FUSION TARGETS

S. H. GLENZER, L. J. SUTER, K. G. ESTABROOK, and H. A. BALDIS
Lawrence Livermore National Laboratory, P.O. Box 808, L-437, Livermore CA 94550

We have applied ultraviolet Thomson scattering to accurately measure the electron and ion temperature in high-density gas-filled hohlraums at the Nova laser facility. The implementation of a short-wavelength probe laser that operates at 263 nm (4ω) has allowed us for the first time to investigate scalings to high gas fill densities and to characterize the hohlraum conditions of the low-Z gas plasma. as well as of the high-Z wall plasma. These measurements have provided us with a unique data set that we use to make critical comparisons with radiation-hydrodynamic modeling using the code LASNEX. This code is presently being applied to design fusion targets for the National Ignition Facility. The Thomson scattering experiments show the existence of electron temperature gradients in the gas plasma that are well modeled when including a self-consistent calculation of magnetic fields. The fields are of relatively small strength not affecting the Thomson scattering spectra directly but limiting the electron thermal transport in the gas resulting into temperature gradients consistent with the experimental observations. In addition, the ion temperature data show that the stagnation time of the gas plasma on the hohlraum axis, which is driven by the radial inward flowing plasma, is sensitive to the gas fill density and is well described by the calculations.

1. Introduction

High-density gas-filled hohlraums[1,2,3] are the baseline targets for indirectly driven inertial confinement fusion (ICF) experiments at future mega-joule laser facilities such as the National Ignition Facility (NIF).[4] They serve as radiation enclosures to convert the high-power laser energy into soft x rays[5,6] which produce a symmetric ablation pressure on the surface of a fusion capsule mounted inside the hohlraum with the goal to achieve high-convergence high-yield implosions.[7,8] The gas fill is important to prevent early axial stagnation of the hohlraum wall blow-off plasma (typically gold) that can cause a localized axial pressure on the fusion capsule deteriorating the symmetry. In addition, it is utilized to reduce inward motion of the gold wall plasma allowing active control of the soft x-ray radiation symmetry.[1,7] In this study, we test the plasma characteristics of this design with Thomson scattering measurements in millimeter-scale hohlraum plasmas providing temporally and spatially resolved measurements of the electron temperature, T_e, ion temperature, T_i, and plasma flow, $\mathbf{v}$. Besides testing our modeling capability, accurate temperature data from Thomson scattering are also needed for calculations of laser scattering losses, beam deflection angles, and the x-ray emission spectra from gas-filled hohlraums.

Predicting hohlraum plasma conditions is an important part of the design work of fusion targets because, e.g., they determine the growth of parametric laser-plasma instabilities, namely stimulated Brillouin scattering (SBS) and stimulated Raman scattering (SRS), which itself limit the range of attainable hohlraum x ray radiation fields (that are characterized by the radiation temperature, T_{RAD}). The hohlraum experiments described in this paper were designed to provide benchmark data for our radiation-hydrodynamic modeling. The hohlraum plasmas were produced at the 30-kJ Nova laser

facility using standard cylindrical millimeter-size gold cavities filled with methane (CH_4) or propane (C_3H_8). These gas fills are characteristic to ignition hohlraums designed for the NIF since they give a two ion species plasma to control ion Landau damping of the ion acoustic plasma waves. This technique might help to reduce laser energy losses by SBS and SRS.[9] In addition, the CH_4-filled hohlraums produce electron densities of 10^{21} cm^{-3} at the peak heater beam intensity of 2×10^{15} W cm^{-2}, values that are identical with the NIF design. Experiments with the higher gas fill density (C_3H_8) were performed to investigate scalings.

For both targets, we find significant electron temperature gradients reaching measured peak temperatures of T_e = 4.5 keV and T_e = 2.6 keV inside of CH_4-filled and C_3H_8-filled hohlraums, respectively. Radiation-hydrodynamic modeling with the code LASNEX[5,10] shows excellent agreement in all cases when accounting self-consistently for all relevant large-scale magnetic field terms.[2] These simulations use no assumptions about heat transport inhibition and provide a clear improvement over modeling with flux limited thermal transport thereby increasing our confidence of the NIF target modeling.

2. Experiment

The experiments were performed with the Nova laser facility at the Lawrence Livermore National Laboratory. It is a Nd:glass laser operating at 1.055 μm (1ω) which can be frequency converted to 2ω or 3ω. The cylindrical hohlraums of 2,750 μm length and of 1,600 μm diameter were heated with ten smoothed 3ω heater beams with a total energy of 27 kJ. The beams were arranged in cones on either side of the hohlraum so that each beam forms an angle of 50° to the hohlraum axis. The heater beams penetrate the hohlraum at both ends through laser entrance holes which are covered with 0.35 μm thick polyimide membranes. We applied shaped laser pulses of 2.4 ns duration which rise from 0.6-1.8 TW per beam reaching peak power at 1.5 ns. We used the 4ω probe laser[11] at Nova for Thomson scattering. In these experiments, the probe was operating at 4ω (λ_0 = 263.3 nm) with a 2 ns long pulse providing 50 J (at 4ω) on target which is not perturbing the hohlraum plasma since this energy is negligible compared to that of the heater beams. We focussed the probe beam to a 100 μm spot inside the hohlraum into the gold blow off plasma at a distance of 300 μm from the hohlraum wall and into the gas plasma on the hohlraum axis. Fig. 1 shows a schematic of the hohlraum and the location of the scattering volumes on a temporal-resolved 2-D x-ray image (E > 2keV) showing the hohlraum emission as observed though the laser entrance hole.

The scattered light has been measured at a scattering angle of θ = 90° through a diagnostic window cut in the side of the hohlraum. We employed f/10 optics with a 1.5 magnification and a 1m spectrometer equipped with an optical streak camera to record spectra with a wavelength resolution of 0.1 nm and a temporal resolution of 30 ps. High spatial discrimination of 133 μm in the vertical direction and 66 μm in the axial direction was obtained by choosing the entrance slit width of the spectrometer to be 200 μm and by employing a streak camera slit height of 100 μm. Collective Thomson scattering is expected for the parameters of the experiments (electron density, temperature,

scattering angle, and probe laser wavelength). Typical scattering parameters are $\alpha = 1/k\lambda_D > 3$, and light is predominantly scattered into the narrow ion feature of the Thomson scattering spectrum.

Figure 1 also shows Thomson scattering data observed from both regions of a C_3H_8-filled hohlraum close to peak heater beam power along with fits of the theoretical Thomson scattering form factor giving T_e in case of the gold plasma, and T_e and T_i in case of the propane plasma. In case of gold, the width of the ion acoustic peak is determined by the detector resolution and by the velocity gradient in the scattering volume along the scattering vector **k**.

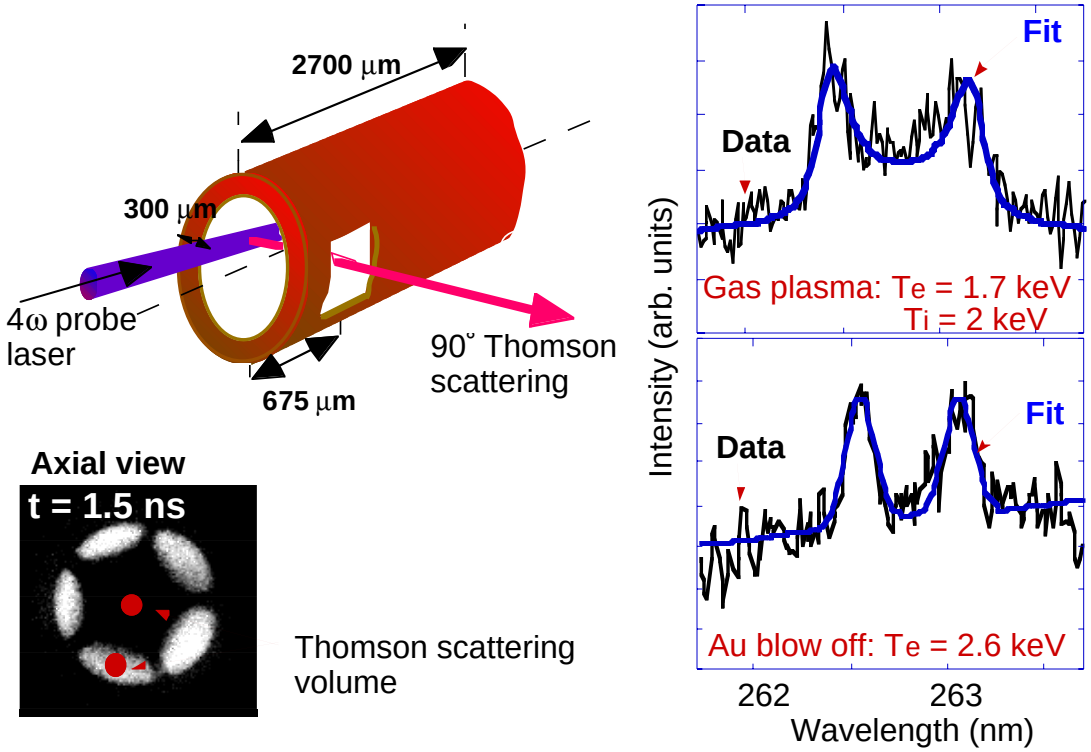

Fig. 1: Schematic of the gas-filled hohlraum Thomson scattering experiment using propane: C_3H_8. The x-ray image indicates the locations of the Thomson scattering volumes and examples of Thomson scattering spectra are shown on the right for scattering from the gas plasma and the gold plasma.

The Thomson scattering spectrum from the low-Z gas plasma, on the other hand, shows broad ion acoustic peaks. This is because the two ion acoustic waves belonging to C and H give rise to four unresolved ion acoustic peaks. Furthermore, ion Landau damping is important for the low-Z species causing an additional broadening of the spectra which is sensitive to T_i. From the spectra we infer the plasma parameters with high accuracy where error bars are obtained by varying the fits within the noise of the experimental data. Electron temperature gradients are also taken into account although they primarily affect the measurement of the ion temperature. A small uncertainty in T_e of about 5% is added due to this effect resulting in a total error bar for T_e of 15%. The error bar for T_i is larger because noise and plasma gradients are more important resulting in an uncertainty of 25%. Finally, the macroscopic plasma flow velocity along the scattering vector **k** is inferred from the Doppler shift of the whole Thomson scattering spectrum away from the incident laser wavelength λ_0. In our experiments, we observe blue shifts at both scattering volumes indicating that the plasma is

moving away from the hohlraum wall and from the hohlraum center towards the laser entrance holes consistent with x-ray imaging and with modeling.

3. Results and Discussions

Figure 2 shows the experimental temperatures measured on the axis at various distances from the hohlraum center. Data are shown from methane-filled hohlraums at t = 1.3 ns and from propane-filled hohlraums at t = 1.4 ns together with results from two-dimensional radiation-hydrodynamic modeling. We applied the code LASNEX with two approximations: The first model uses a flux-limited diffusion model for heat transport where the heat flow per unit area in regions of large classical heat flow $\kappa \nabla T_e$ has an upper bound of f (n_e T_e v_e) where (n_e T_e v_e) is the so-called free streaming value of heat transport and f is the flux limit chosen to be f = 0.05. The second model includes large-scale magnetic fields.[2]

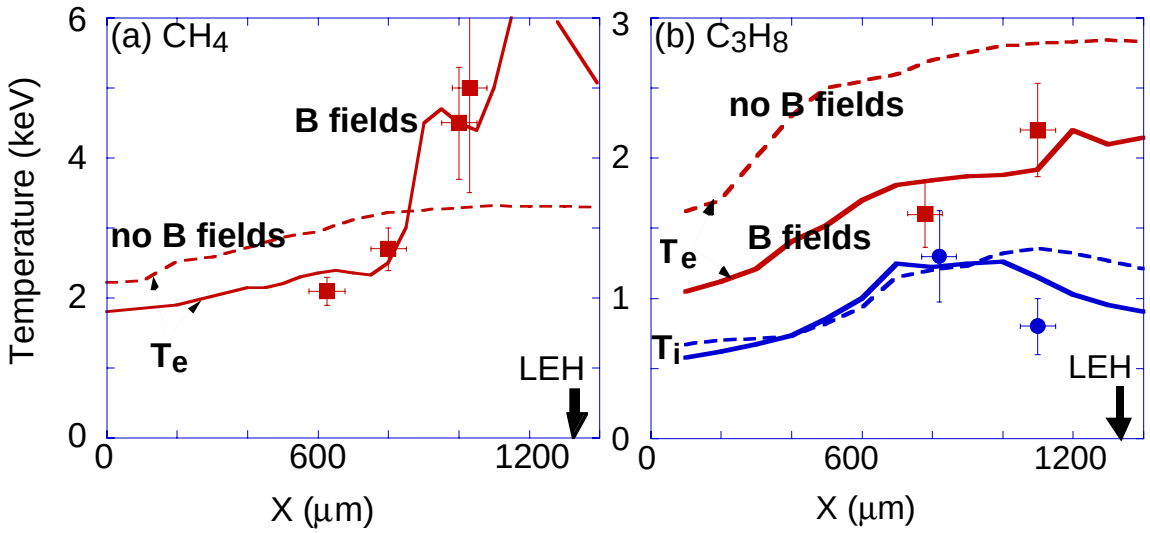

Fig. 2: Hohlraum axial T_e (squares) and T_i (circles) data as function of distance from the hohlraum center for (a) methane gas fill at t = 1.3 ns and (b) propane gas fill at t = 1.4 ns together with hydrodynamic simulations with two electron heat transport models. In (a), the T_i data are close to 3 keV and are removed for clarity since they overlap with the T_e data points.

Our magnetic field solution goes beyond the magnetohydrodynamic (MHD) limit since the full Maxwell field equations are solved, including the displacement current so that charge separation is included. A generalized Ohm's law defines the current density. In the co-moving fluid frame the current density (in Gaussian units) obeys the following equation:

$$\partial \mathbf{J} / \partial t + \mathbf{J} \times \Omega = e/m_e \nabla P_e + \omega_p^2/4\pi \quad \mathbf{E} + \mathbf{R}, \qquad (1)$$

where Ω is the electron cyclotron frequency, P_e is the electron pressure, **E** is the electric field, and the other symbols have their usual meanings. **R** is related to the collisional contribution to the momentum

flux that is given in Ref. 12 as a constitutive relation relating the drift velocity and the electron temperature gradient to the momentum flux and, hence, the electric current. The various terms which contribute to the generation of large-scale magnetic fields can be found by solving Eq. (1) for the electric field and substituting into Faraday's law. Some of the terms which result are: the ∇T_e x ∇n_e source term, magnetic convection, resistive diffusion, magnetic curvature, magnetic pressure, and thermal force terms. These terms are all of the same order and must all be included in the simulations. Magnetic fields produced by hot electrons are not included as well as small-scale fields of the size of laser filaments. The calculated temperatures shown in Fig. 2 are taken along the axis averaged over 60 μm consistent with the size of the scattering volume. This comparison is justified because the probe beam is not affected by beam deflection or refraction.

The comparison in Fig. 2 clearly shows that the inclusion of magnetic fields into the modeling results in excellent agreement between the Thomson scattering data and the calculations. At early times, magnetic fields of the order of 1 MG are produced at the hohlraum walls where the laser beams initially deposit their energy. In addition, the hohlraum window is also magnetized. These fields convect into the low-Z plasma of the hohlraum causing inhibition of electron thermal conduction since the product of the electron cyclotron frequency and electron-ion collision time $\omega_e\tau_e$ approaches values of ten (for $\omega_e\tau_e$~1, thermal conduction effects become important). In particular, hot plasma regions develop in the path of the laser beams which are surrounded by large magnetic fields. Furthermore, temperature gradients develop along the axis of the hohlraum and are clearly correlated to the presence of the magnetic fields. Our Thomson scattering measurements have observed both regions of hot plasma, the hot off-axis regions (Ref. 2) and the axial temperature gradient (Fig. 2). The good agreement of this model with the Thomson scattering data is very encouraging as its demonstrates our level of theoretical understanding of hohlraum plasma conditions and electron thermal transport as well as the importance of magnetic fields in ICF hohlraums. Our measurements in the higher density gold blow off also agree slightly better with the calculations that include magnetic fields compared to those without magnetic fields, although the latter are still within the error bar of the experiment. It indicates that magnetic fields do not affect the radiation production of these hohlraums. Indeed, the LASNEX simulations with B fields average 3 eV higher than those without fields which is indistinguishable with present radiation drive measurement techniques. However, the simulations with B fields are important to predict the plasma conditions of ICF targets. They are presently used to develop our understanding of laser scattering losses by SBS and SRS in hohlraums. For example, we find that SRS spectra, calculated from a convective gain model with LASNEX calculations providing the input plasma parameters, show improved agreement when including magnetic fields.

Figure 2 (b) further indicates that the ion temperatures are less sensitive to the heat transport model used in the simulations since they are determined by p dV-work when the low-Z plasma is compressed on the axis by the inward blowing gold plasma from the hohlraum walls. In case of methane, the experimental ion temperatures rise rapidly at t = 1.2 ns to peak values of T_i = 3 keV. The hydrodynamic simulations confirm that the rise of T_i is due to stagnation of the compressed low-

Z plasma on the axis of the hohlraum where 90˚ particle scattering occurs on a scale length of 30 μm. When increasing the gas fill density by more than a factor of two using C_3H_8, Thomson scattering shows that the stagnation time is delayed by 0.3 ns. This finding is in good agreement with the radiation-hydrodynamic calculations verifying that a higher density gas fill in ignition target designs will be beneficial in preventing early axial stagnation.

4. Conclusions

Our Thomson scattering experiments at Nova have changed the way we model laser fusion plasmas. They have shown the need to take into account heat transport limiting effects such as magnetic fields to model the conditions in ICF plasmas. The present experiments have pushed the limits of the applicability of Thomson scattering to a parameter range of $1\text{eV} < T_e < 5$ keV and 10^{11} cm^{-3} $< n_e <$ 3×10^{21} cm^{-3}. Our results have shown steep electron temperature gradients in hohlraums which are modeled well by radiation-hydrodynamic simulations when including magnetic fields. The measurements in the gold blow off recently became feasible due to the development of the 4ω probe laser. The data will be used in future studies to further test radiation physics models. Moreover, the measurements of the ion temperature have shown that axial stagnation in these gas-filled hohlraums is well described by the simulations. In particular, the experimental data show a scaling of the stagnation time to higher gas fill densities consistent with the calculations which emphasizes that the gas fill will be an efficient tamper for future ICF experiments.

Acknowledgments

We would like to thank B. J. MacGowan, W. Rozmus, and P. E. Young for discussions. This work was performed under the auspices of the U.S. Department of Energy by the Lawrence Livermore National Laboratory under contract No. W-7405-ENG-48.

References

1. J. D. Lindl, Phys. Plasmas **2**, 3933 (1995).
2. S. H. Glenzer *et al*., Phys. Rev. Lett. **79**, 1277 (1997). Phys. Plasmas **6**, 2177 (1999).
3. S. H. Glenzer *et al*., Phys. Rev. Lett. **80**, 2845 (1998).
4. J. A. Paisner *et al*., Laser Focus World **30**, 75 (1994).
5. L. J. Suter *et al*., Phys. Rev. Lett. **73**, 2328 (1994). Phys. Plasmas **3**, 2057 (1996).
6. R. L. Kauffman *et al*., Phys. Rev. Lett. **73**, 2320 (1994). Phys. Plasmas **5**, 1927 (1998).
7. S. W. Haan *et al*., Phys. Plasmas **2**, 2480 (1995).
8. W. J. Krauser *et al*., Phys. Plasmas **3**, 2084 (1995).
9. R. K. Kirkwood *et al*., Phys. Rev. Lett. **77**, 2706 (1996). Phys. Plasmas **4**, 1800 (1997).
10. G. B. Zimmerman and W. L. Kruer, Comments Plasma Phys. Controlled Fusion **2**, 85 (1975).
11. S. H. Glenzer, *et al*., Rev. Sci. Instrum. **70**, 1089 (1999).
12. S. I. Braginskii, in Reviews of Plasma Physics, ed. M. A. Leontovitch (Consultants Bureau, New York, 1965), Vol. 1, p. 205.